



# Biological Characterization and Pluripotent Identification of Cartilage Stem/Progenitor from Peking Duck

Xibin Liu<sup>1,2,3</sup>, Weijun Guan<sup>2,\*</sup> and Dong Zheng<sup>1,\*</sup>

<sup>1</sup>College of Wildlife and Protected Area, Northeast Forestry University, Harbin, 150040, China

<sup>2</sup>Institute of Animal Sciences, Chinese Academy of Agricultural Sciences, Beijing, 100193, China

<sup>3</sup>Graduate Management Division, Student Affairs Office, Yantai University, Yantai, 264005, China

## ABSTRACT

A group of cells in cartilage tissue with stem cell characteristics may be ideal seed cells for cartilage defect repair. In previous studies, stem/progenitor cells from articular cartilage have been isolated and identified in humans, horses, and bovines, but rarely in ducks. We isolated and cultured cartilage stem/progenitor cells (CPSCs) from the articular cartilage of 14-day-old Peking duck embryos using the fibronectin adhesion method. The morphology of CPSCs was observed under an inverted microscope. Based on the growth curve test, we found that the growth mode of the cells was “S” type growth. The clonogenic assay was performed to determine the clonogenic efficiency CPSCs. The expression of cell surface markers was detected by immunofluorescence, flow cytometry, and RT-PCR, and it was found that the CPSCs positively expressed FGFR-3, collagen type II, CD44, CD73, CD90, vimentin, Notch1, CD105, and CD106, but negatively expressed the haematopoietic stem cell surface marker CD34. Furthermore, CPSCs were successfully induced to differentiate into adipocytes, osteoblasts, and chondrocytes, showing that they have an *in vitro* differentiation ability. These findings provide a theoretical and experimental basis for cell transplantation therapy in tissue engineering.

## Article Information

Received 22 December 2020

Revised 28 January 2021

Accepted 01 February 2021

Available online 25 February 2022 (early access)

Published 24 October 2022

## Authors' Contribution

XL performed the experiments and drafted the manuscript. WG wrote and reviewed the manuscript. DZ conceived the study and participated in its design and coordination.

## Key words

Peking duck, Cartilage stem/progenitor, Biological characterization, Directional differentiation.

## INTRODUCTION

There are three types of cartilage tissues in the human body: hyaline cartilage, fibrocartilage, and elastic cartilage, which can be distinguished by their unique molecular compositions. Articular cartilage, *i.e.* hyaline cartilage that covers the end of joints, is a non-vascular, non-neural tissue with a high degree of extracellular matrix and cell ratio; chondrocytes have always been considered the only cell type in articular cartilage (Tang *et al.*, 2019). Articular cartilage is a non-self-repairing tissue. Injury of cartilage often marks the initiation of tissue degeneration, and the progressive cartilage loss and subchondral bone sclerosis lead to degenerative joint diseases. Cartilage defects caused by various diseases and trauma represent

a clinical problem (Jungmann *et al.*, 2013; Pei *et al.*, 2013; Reverte-Vinaixa *et al.*, 2013). However, cartilage tissue engineering provides a new method for the repair of cartilage tissue defects (Naderi-Meshkin *et al.*, 2014; Viti *et al.*, 2014). Seed cells have become one of the most important factors restricting the clinical application of cartilage tissue engineering. Chondrocytes are the first seed cells to be used in cartilage tissue engineering research; however, they can only be isolated from a limited number of sources, have a slow proliferation rate *in vitro*, and dedifferentiate easily. Thus, they are not ideal seed cell candidates (Kreuz *et al.*, 2013). Stem cells not only show pluripotency and unlimited self-renewal, but also have the ability to differentiate into at least one specific tissue (Puculek *et al.*, 2020). In addition, stem cells are advantageous in that they can be easily extracted, and show strong proliferation ability and multi-directional differentiation potential. Researchers are gradually focusing on adult stem cells, and have used bone marrow mesenchymal stem cells (BMSCs) or adipose-derived mesenchymal stem cells (ADSCs) to construct tissue-engineered cartilage to repair cartilage defects (Diekmann *et al.*, 2012; Veronesi *et al.*, 2014). However, further studies have found that problems such as “vascularization” and “ossification” appeared after chondrocytes obtained

\* Corresponding authors: [weijunguan301@gmail.com](mailto:weijunguan301@gmail.com);

[zhengdong89@yeah.net](mailto:zhengdong89@yeah.net)

0030-9923/2023/0001-213 \$ 9.00/0



Copyright 2023 by the authors. Licensee Zoological Society of Pakistan.

This article is an open access article distributed under the terms and conditions of the Creative Commons Attribution (CC BY) license (<https://creativecommons.org/licenses/by/4.0/>).

by the differentiation of BMSCs were transplanted onto the skin of nude mice (Pelttari *et al.*, 2006; Cui *et al.*, 2007). Moreover, cartilage constructed from adipose-, synovial-, and periosteal-derived stem cells is also associated with defects such as cartilage dysfunction (Peng and Huard, 2004). Thus, these stem cells are not ideal seed cells for cartilage tissue engineering. However, many studies have reported that a group of cells with stem cell characteristics exist in cartilage tissue; these may be ideal seed cells for cartilage defect repair (de Luca *et al.*, 2019). Such cells have a self-proliferation ability, surface antigen-expression characteristics, and multi-directional differentiation potential. Human articular chondrocytes were dedifferentiated by monolayer culturing, and a small fraction of these cells still has the ability to form clones and show multi-directional differentiation (osteogenesis, chondrogenesis, and adipogenesis). The articular cartilage mesenchymal progenitor cells in normal and osteoarthritic cartilage tissues, based on the co-expression of the cell surface markers CD105 (endothelin) and CD166 (activated leukocyte adhesion molecule) (Alsalameh *et al.*, 2004). These cells are comparable to BMSCs with regards to their ability to differentiate into adipocytes or osteocytes. Several independent research groups have reported the presence of stem or progenitor cells in human articular cartilage tissues. Derived from human late-stage osteoarthritic cartilage tissues which have migration ability and the expression of many surface markers in these cells are similar to that in mesenchymal stem cells. Until now, CPSCs have been observed in human, horse, and bovine articular cartilage; they have been identified, isolated, and characterized for their ability to self-renew, express stem cell-associated surface markers, and differentiate into multiple lineages. However, there are few articles on obtaining CPSCs from poultry, which are commonly found organisms.

## MATERIALS AND METHOD

### *Experimental animals and reagents*

Fertilized eggs were provided by the Peking duck breeding farm of the Chinese Academy of Agriculture Science, Beijing, China. Animal experiments were performed in accordance with the guidelines established by the Institutional Animal Care and Use Committee at the Chinese Academy of Agricultural Sciences.

The following materials were used in this study: epidermal growth factor (EGF), basic fibroblast growth factor (bFGF), and transforming growth factor-beta 3 (TGF- $\beta$ 3), which were purchased from Peprotech (Rocky Hill, TX, USA); foetal bovine serum (FBS), Dulbecco's modified Eagle's medium/F12 (DMEM, Gibco, USA); isobutyl methylxanthine (IBMX),  $\beta$ -glycerophosphate,

dexamethasone, Vitamin C (VC), indomethacin, insulin, sodium pyruvate 4',6-diamidino-2-phenylindole (DAPI), and L-proline, which were purchased from Sigma-Aldrich (St. Louis, MO, USA); rabbit antibodies against CD29, CD34, CD90, CD105, CD106, fibroblast growth factor receptor 3 (FGFR-3), and collagen type II; fluorescein isothiocyanate (FITC)-conjugated goat anti rabbit IgG (secondary antibody) was purchased from Bioss (Beijing, China).

### *Isolation and culture of CPSCs*

Peking duck articular cartilage tissues were isolated under aseptic conditions; they were washed seven times with phosphate buffered saline (PBS) containing 100 U/ml penicillin and 100 mg/ml streptomycin and cut into pieces. The cartilage fragments were digested with 0.02% type II collagenase for 4 h in a cell culture incubator and were shaken once every 30 min to allow them to be fully digested. After the digestion was stopped using culture medium, the mixtures were filtered through a 74- $\mu$ m-mesh sieve and then centrifuged at 200 g for 8 min at 25°C. The digested cells were resuspended in PBS, and inoculated into a 6-well plate containing fibronectin, followed by incubation overnight at 4°C. After 20 min, the cell suspension was aspirated and added to the medium (DMEM/F12 and 10% (v/v) FBS). The supernatant was discarded, and the pellet was resuspended in complete medium consisting of DMEM/F12 with 10 ng/mL EGF, 10 ng/mL bFGF, 10% (v/v) FBS, and 100 IU/mL penicillin/streptomycin. CPSCs were attached to the bottom of the cell culture dish, and the medium was changed after 24 h.

### *Growth kinetics*

CPSCs from passages 3, 15, and 25 (P3, P5, and P25, respectively) were collected and plated in 24-well microplates at a density of  $10^4$  cells/ml. After plating, the cells from three wells were counted using a blood cell-counting plate at the same time every day; this process was repeated consecutively for eight days. The number of cells in each well was counted thrice to calculate the mean values, which were used to plot the growth curve. The population doubling time (PDT) was calculated based on the formula  $PDT = (t - t_0) \lg 2 / (\lg N_t - \lg N_0)$  ( $t_0$  is starting time of culture;  $t$  is termination time of culture;  $N_t$  is ultimate cell number in the culture;  $N_0$  is initial cell number in the culture).

### *Colony formation assay*

CPSCs from P3, P15, and P25 were plated in 60-mm plates at a density of 100 cells per plate. After seven days of culture, the colonies formed were stained with Giemsa, and the number of colony forming units was counted. The cloning efficiency was calculated as: (number of colony forming units/number of starting cells)  $\times$  100%.

**Table I.- Primer sequences used in RT-PCR assay.**

Gene name	Primer sequences	Product length (bp)	T <sub>m</sub> (°C)
GAPDH	F:5'-GCCTGGAAAAACCAGCCAAG-3' R:5'-GGGAACAGAACTGGCCTCTC-3'	378	60
CD44	F:5'-AGCTGGAAAAAGCTCACGAA-3' R:5'-GGACTGGATCTCCTGATGGA-3'	400	56
CD73	F:5'-ACCTGCTCTGTGATGCTGTG-3' R:5'-AGCATGTGGTAGCCATCTCC-3'	451	60
CD90	F:5'-CAGTGCCAGATGATCAAGGA-3' R:5'-CACAGGGACACGAAGTCCACT-3'	434	56
Vimentin	F:5'-ACTCCAGGAACAGCACATCC-3' R:5'-CTCCCTCCAGCAGTTTTCTG-3'	476	57
Notch1	F:5'-AAGTTCAGGTTTCGAGGAGCA-3' R:5'-GGTTGCCCTGTTCCCTAATGA-3'	495	60
ACAN	F:5'-GAGCTGTACGAGGGCTTCAC-3' R:5'-AGCTCTCCTTGTCTCCACA-3'	547	58
OPN	F:5'-TTGTGGATGACGACAACGAT-3' R:5'-GTTGCTGGTGTCAATGG-3'	554	58
RUNX2	F:5'-CGCATTCTCATCCAGTAT-3' R:5'-TATGGAGTGTGCTGGTCTG-3'	515	60
ALP	F:5'-CCTACACGGCTCTCTCCAAG-3' R:5'-TTGGGATACTCAGGGTCTGG-3'	439	58
LPL	F:5'-GCTGGTCCCACCTTTGAGTA-3' R:5'-CTTCTGGCAATGTGAAAGCA-3'	595	60
PPAR $\gamma$	F:5'-TCAGAAATGCCTTGCTGTTG-3' R:5'-CTCCCGTGTCATGAAACCTT-3'	553	60

*Immunofluorescence of CPSC surface markers*

CPSCs from P3 were fixed in 4% paraformaldehyde for 15 min and subsequently washed thrice in PBS. They were then permeabilized with 0.25% Triton X-100 for 20 min and washed thrice with PBS. The samples were then blocked with goat serum for 30 min, and subsequently incubated with the following primary antibodies (1:200 dilution): rabbit anti-FGFR-3, rabbit anti-collagen type II, rabbit anti-CD105, rabbit anti-CD106, and rabbit anti-CD34 overnight at 4°C. The cells were then washed thrice with PBS and incubated with FITC-conjugated secondary antibodies for 1 h at room temperature in the dark. After incubation, the cells were washed thrice with PBS and then counterstained with DAPI in the dark. Finally, the cells were washed thrice with PBS and examined under a confocal microscope (Nikon, Tokyo, Japan).

*Flow cytometry analysis*

CPSCs from P3 were collected in centrifuge tubes at a density of  $1 \times 10^6$  cells per tube. Then, the cells were centrifuged at 400 g for 10 min and fixed using 70% (v/v) ethanol on ice overnight at 4°C. They were then centrifuged again at 200 g for 8 min and blocked with goat serum. Next, the cells were incubated with primary antibodies

(1:200 dilution) overnight at 4°C. The following antibodies were used: rabbit anti-CD29, rabbit anti-CD90, rabbit anti-CD105, and rabbit anti-CD106. The primary antibodies were replaced with PBS in case of the negative control. The samples were then washed with PBS and incubated with FITC-conjugated goat anti-rabbit secondary antibodies for 1 h at room temperature. Finally, they were washed in PBS and subjected to fluorescence-activated cell sorting (FACS) analysis using a single channel.

*RT-PCR analysis*

RNA was extracted from the cells using the Trizol reagent (Invitrogen, Carlsbad, CA, USA), and cDNA was synthesized using a reverse transcription system (Tiangen, Beijing, China). The cDNA targets were amplified by PCR using specific primer pairs, and the PCR products were visualized by electrophoresis on a 2% agarose gel. The gene-specific primers were designed using the Primer Premier 5.0 software (Premier Biosoft, Palo Alto, CA, USA); they are listed in Table I.

*Differentiation of CPSCs in vitro*

We tested the osteogenic, chondrogenic, and adipogenic differentiation ability of the CPSCs. After

achieving 60–80% confluence, the cells from P3 were divided into two groups, the induction group and the

control group, and cultured using different media. The medium was changed every two days.

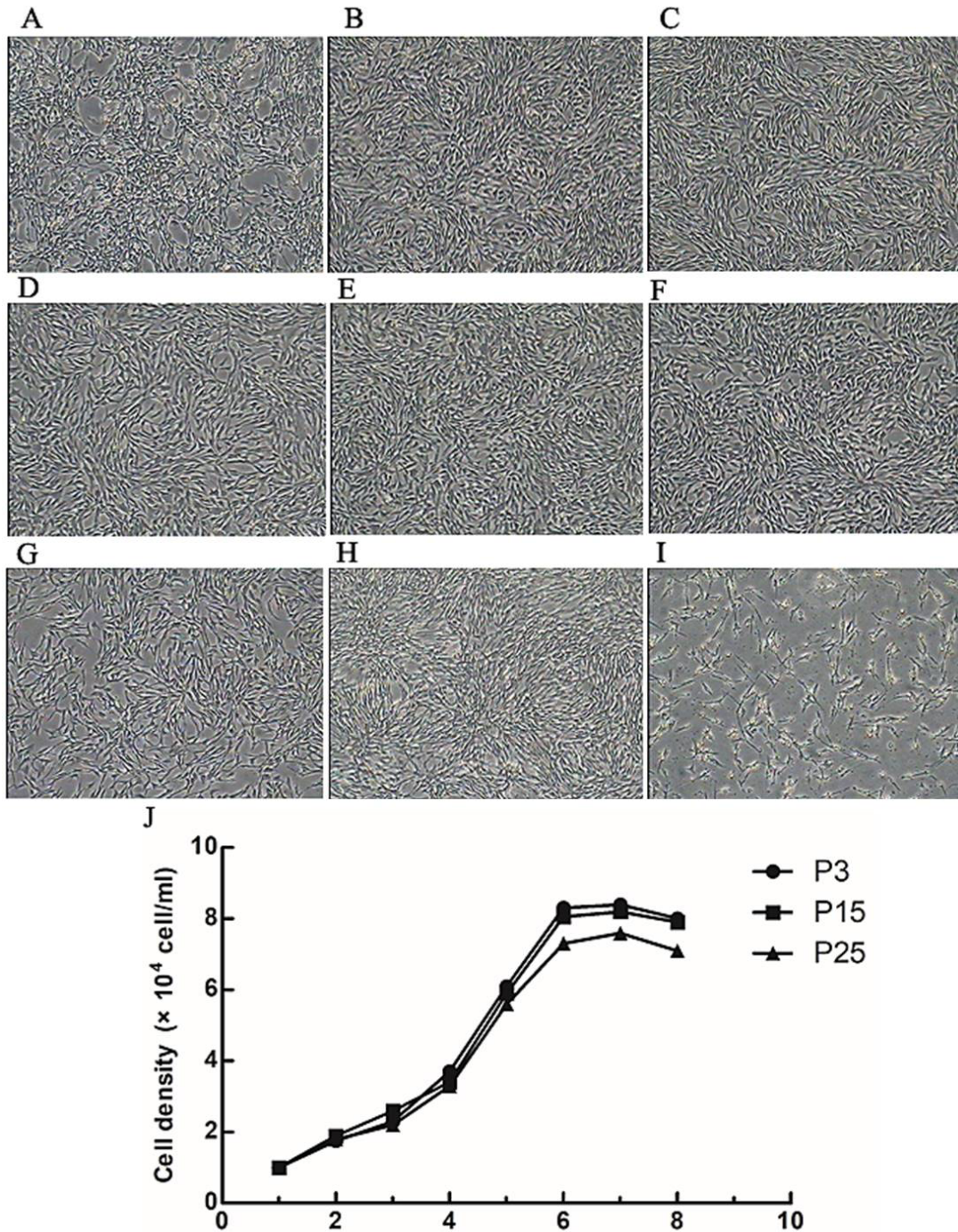


Fig. 1. Morphology of primary cultured and sub-cultured CPSCs. **A–I**, representative cellular morphologies of CPSCs from passage 0, 1, 3, 5, 10, 15, 20, and 25, respectively (40 $\times$ ). **J**, the growth curves of CPSCs from P3, P15, and P25 were all typically sigmoidal; the cell density is reflected by the vertical axis. The growth curves consist of the latent period, logarithmic period, stable period, and decline period. The population doubling times (PDTs) during the logarithmic, stable, and decline periods were about  $39.66 \pm 9.11$  h,  $40.38 \pm 8.89$  h, and  $43.06 \pm 8.84$  h, respectively.

#### *Osteogenic differentiation of CPSCs*

CPSCs in the induced group were cultured in osteogenic medium, which consisted of DMEM/F12 medium supplemented with 10% FBS, 0.1  $\mu$ M dexamethasone, 10 mM  $\beta$ -glycerophosphate, and 0.1 mM VC. CPSCs in the control group were maintained in standard culture medium without any inducers of differentiation. Two weeks later, the cells' capacity for calcium node formation was detected by Alizarin Red staining; osteoblast-specific genes were further detected by RT-PCR.

#### *Chondrogenic differentiation of CPSCs*

CPSCs in the induced group were cultured in chondrogenesis medium, which consisted of DMEM/F12 medium supplemented with 5% FBS, 0.1 mM dexamethasone, 1% ITS (Insulin, Transferrin, Selenium Solution), 50  $\mu$ g/mL L-proline, 0.9 mM sodium pyruvate, 50  $\mu$ g/mL VC, and 10 ng/mL TGF- $\beta$ 3. CPSCs in the control group were maintained in standard culture medium. After 15 days, chondrocytes were identified by staining with alcian blue; chondrocyte-specific genes were further detected using RT-PCR.

#### *Adipogenic differentiation of CPSCs*

CPSCs in the induced group were cultured in

adipogenic medium, which consisted of DMEM/F12 medium supplemented with 10% FBS, 1.0  $\mu$ M dexamethasone, 200  $\mu$ M indomethacin, 0.5 mM IBMX, and 10 mg/l insulin. CPSCs in the control group were maintained in standard culture medium. After 14 days, intracellular lipid accumulation in the two groups was identified by staining with oil red O; lipocyte-specific genes were further detected by RT-PCR.

## RESULTS

#### *Morphology of CPSCs*

In primary culture, the CPSCs showed a fusiform, round, or irregular morphology. After 48 h, the cells showed a fibroblast-like morphology and proliferated rapidly. At 80% confluence, the cells were dissociated using 0.25% trypsin and 0.02% EDTA treatment and cultured in order to obtain a sufficient number of cells. After the primary culture, the cells grow rapidly and new cells are produced every one or two days. After being cultured to the 5th generation, the CPSCs showed a uniform, spindle-shaped, or polygonal morphology. As the number of passages increases, most cells develop senescence, which is detected based on observations such as the presence of vesicles and nuclear pyknosis. Until the cells reached the 29<sup>th</sup> generation, they were detached from the plate (Fig. 1).

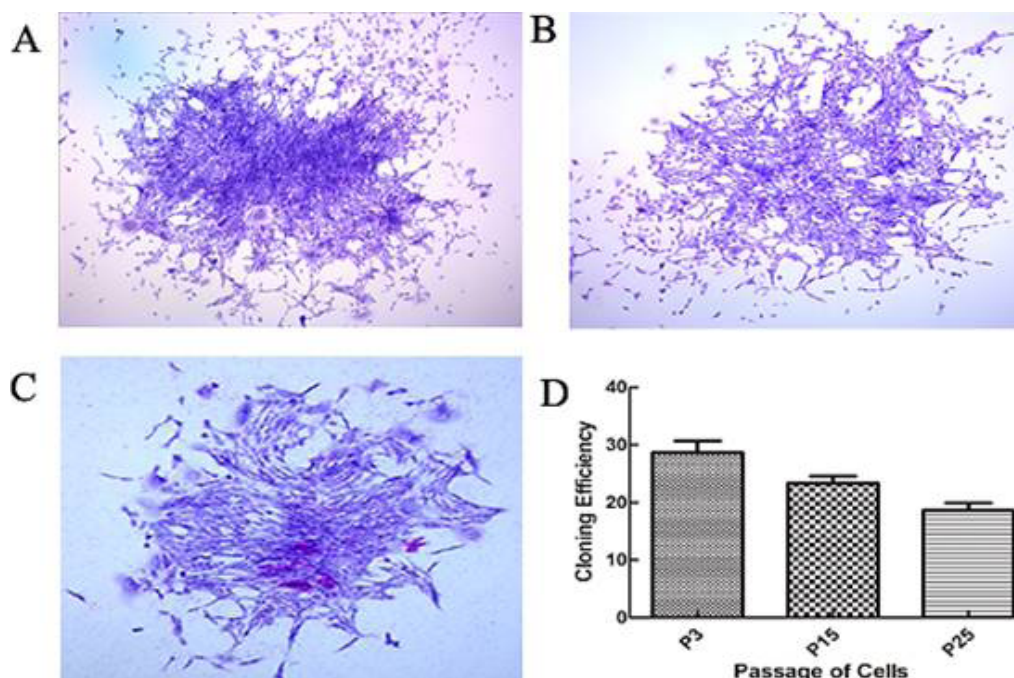


Fig. 2. Cloning efficiency of CPSCs. A–C, morphology of colonies formed by CPSCs from P3, P15, and P25 after 7 days of culture (100 $\times$ ). D, bar chart showing the cloning rates for CPSCs from P3, P15, P25; the colony-forming levels were 28.67  $\pm$  2.87%, 23.33  $\pm$  1.7%, and 18.67  $\pm$  1.7%, respectively.

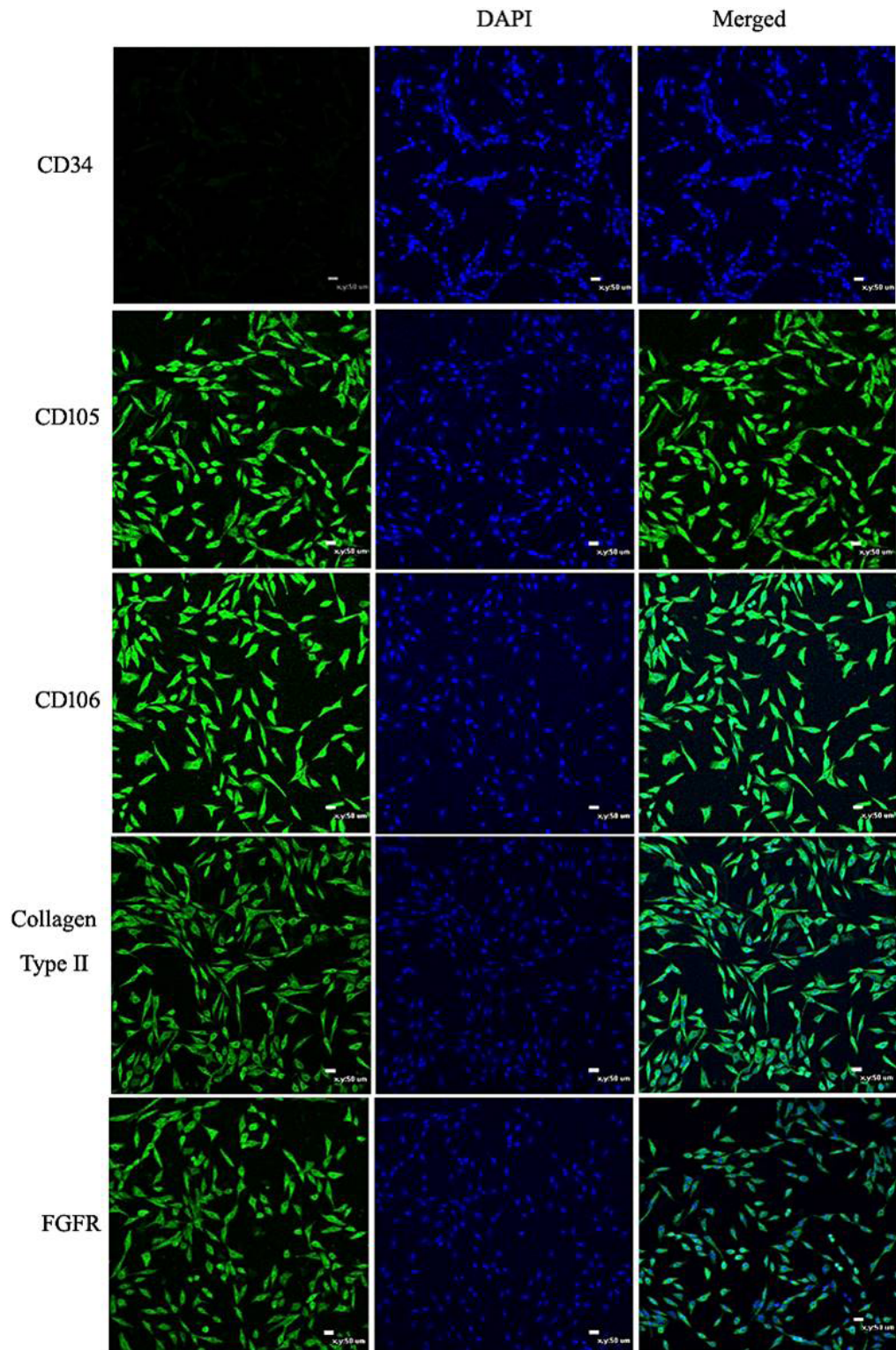


Fig. 3. Immunofluorescence of CPSC surface markers. Cell nuclei stained with DAPI are shown in the middle panels. The pictures shown above indicate that the CPSCs positively expressed FGFR-3, collagen type II, CD105, and CD106, and negatively expressed CD34 (Scale bar = 50  $\mu$ m).

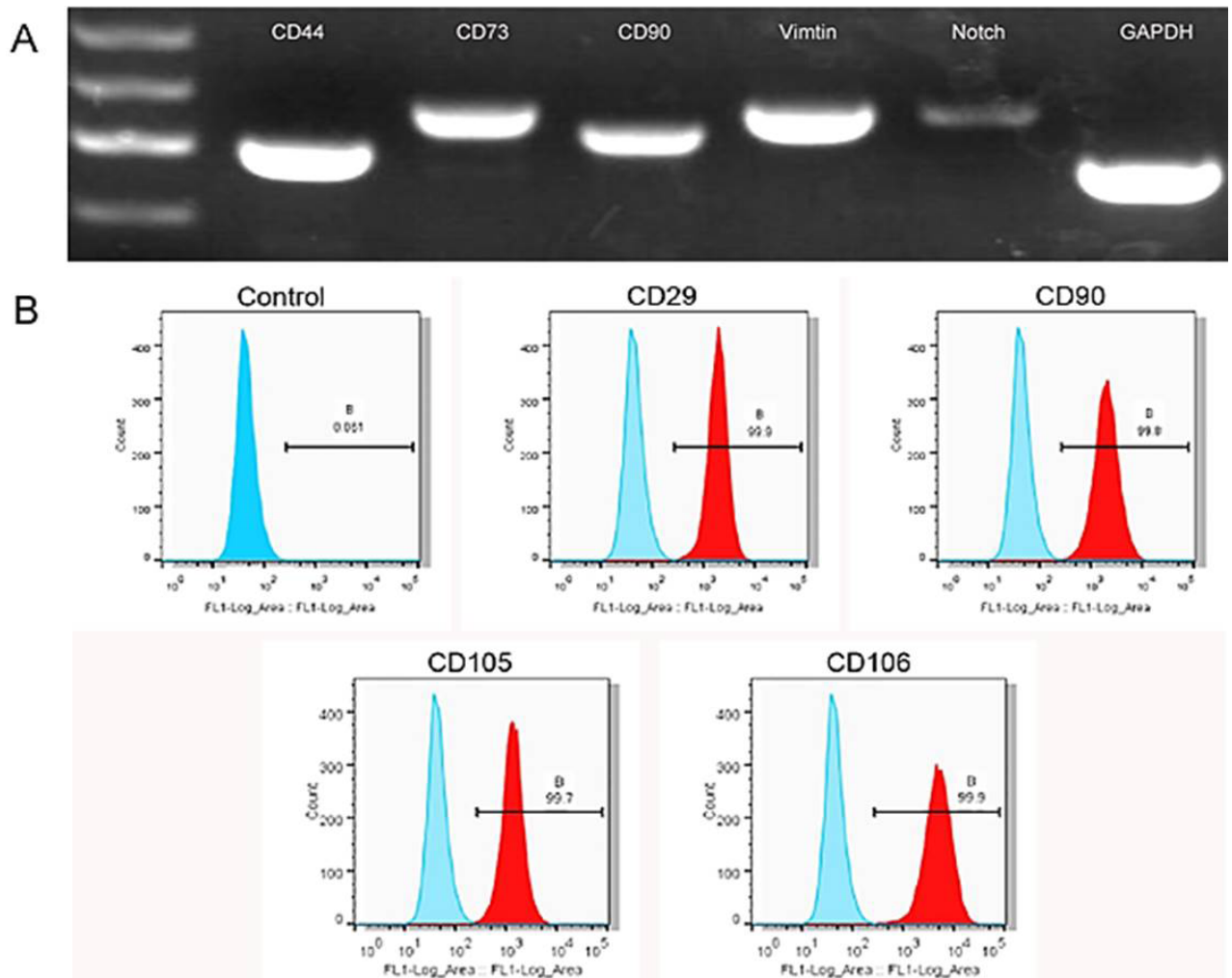


Fig. 4. Detection of CPSC markers by RT-PCR. **A**, the image shows the expression levels of CD44, CD73, CD90, Vimentin, Notch1, and GAPDH. **B**, detection of CPSC markers by flow cytometry. CPSCs were labelled by the markers CD29, CD90, CD105, and CD106. The positivity rates of the CPSCs for all these markers were above 99%.

#### Growth kinetics

CPSCs from P3, P15, and P25 were counted to analyse their proliferation rates. Based on the cell number on each day, the growth curve was drawn using GraphPad Prism (GraphPad Software, Inc., San Diego, California, USA), as shown in Figure 1J. The proliferation curve reveals that the growth showed an S-shape-like tendency, comprising the latent period, logarithmic period, the stable period, and the decline period. After being passaged, the cells entered the latent phase. About 48 h later, the cells began to enter the logarithmic growth phase. During this period, the proliferation ability of the cells was stronger, and their numbers increased logarithmically. When the proliferation and death of the cells reached an equilibrium, the cells entered the stable phase of growth. After the

stationary phase, the number of cells gradually decreased, and the cells entered a recession period of growth. The population doubling times were about  $39.66 \pm 9.11$  h,  $40.38 \pm 8.89$  h, and  $43.06 \pm 8.84$  h during the logarithmic, stable, and decline periods of growth, respectively. Thus, cell proliferation gradually weakened with the increase of the cell passage number (Fig. 1J).

#### Cloning efficiency

Colony formation was observed by microscopy after seven days. The colony-formation efficiencies were  $28.67 \pm 2.87\%$ ,  $23.33 \pm 1.7\%$ , and  $18.67 \pm 1.7\%$  for the cells from P3, P15, and P25, respectively, demonstrating the self-renewal capacity and stem cell characteristics of the cultured CPSCs (Fig. 2).

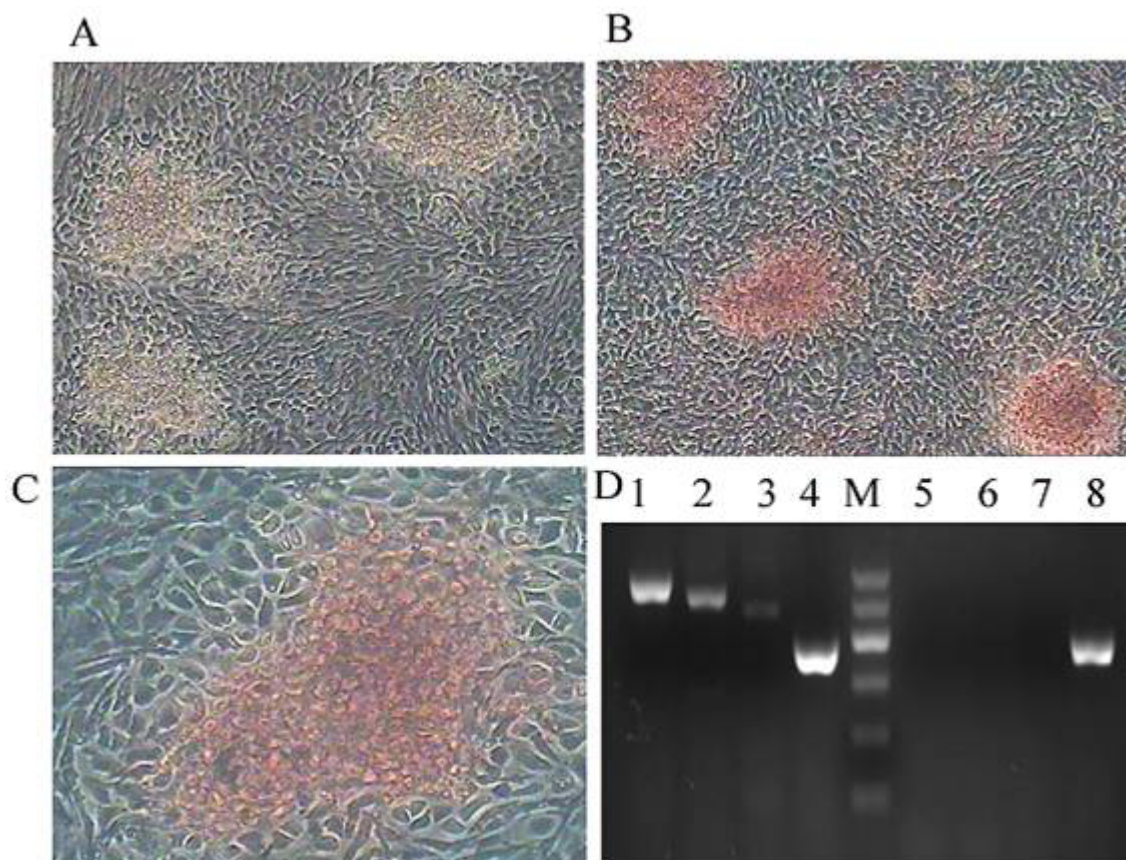


Fig. 5. Osteogenic differentiation of CPSCs. After induction for 14 days, the morphology of the cells changed significantly, from a fusiform appearance to a larger size and more polygonal shape. **A–C**, the induced cells were alizarin red positive (100 $\times$ ). **D**, RT-PCR revealed the expression of the osteoblast-specific genes lane 1 OPN, lane 2 Runx2, lane 3 ALP, GAPDH (lane 4 and lane 8) in cells from the induced group, whereas these genes were not expressed in cells from the control group (lane 5–7). GAPDH served as the internal control.

#### Markers of CPSCs

The CPSC-specific surface markers were detected by immunofluorescence staining (Fig. 3) and RT-PCR (Fig. 4A). The results showed that CD44, CD73, CD90, CD105, CD106, FGFR-3, collagen type II, vimentin, and Notch1 were positively expressed, but CD34 was not. These results were similar to previous data on the characterization of CPSCs *in vitro*. In addition, the positivity rates of these surface markers were detected by flow cytometry, which represented that the CPSCs showed a high expression of CD29, CD90, CD105, and CD106, and the positivity rates for all these markers were above 99% (Fig. 4B).

#### Differentiation of CPSCs *in vitro*

##### Osteogenic differentiation of CPSCs

From the third day of induction, the morphology of some cells changed considerably from a fusiform

appearance to a larger size and more polygonal shape. Over time, the number of triangular or polygonal cells increased, showing growth in multiple layers, and the crystalline particles became apparent. At 14 days of induction, the number of nodules in the cultured cells gradually increased, and the cells were positively stained by alizarin red. Early osteogenic index (alkaline phosphatase, ALP), late osteogenic index (osteopontin, OPN), and osteogenic-specific transcription factors that play an important role in regulating osteoblast differentiation and bone formation (runt-related transcription factor 2, Runx2) were tested by RT-PCR; the cells in the induced group were confirmed to show a positive expression, while those in the control group showed a negative expression of these genes (Fig. 5).

##### Chondrogenic differentiation of CPSCs

From a few days after induction, the proliferation of CPSCs gradually increased. Subsequently, cells in some

areas aggregated to form clusters and became larger. At this time, the rate of proliferation continues to spread at a relatively low rate. After 15 days of induction, the cells were positively stained by alcian blue. Chondrocyte-specific genes, vimentin (VIM) and aggrecan (ACAN), were tested by RT-PCR; the cells in the induced group were confirmed to show a positive expression, while those in the control group showed a negative expression of these genes (Fig. 6).

#### Adipogenic differentiation of CPSCs

From the third day after induction, many bright lipid droplets were observed in the cells. Over time, the number of droplets increases, and the droplets aggregate to form larger droplets. After 14 days of induction, the cells were positively stained by oil red O. Early markers of adipocyte differentiation (lipoprotein lipase, LPL) and an important marker for the degree of adipocyte differentiation (peroxisome proliferator-activated receptor gamma,

PPAR $\gamma$ ) were tested by RT-PCR; the cells in the induced group were confirmed to show positive expression, while those in the control group showed a negative expression of these markers (Fig. 7).

## DISCUSSION

Since stem cells can specifically express fibronectin receptors, we used the fibronectin adhesion method to separate a group of cells from the articular cartilage tissues of Peking duck embryos, indicating that there are stem/progenitors with multi-directional differentiation potential in cartilage tissues. This method was first used by Jones *et al.* to sort epidermal stem cells. The principle is that stem cells can specifically express the fibronectin receptor, integrin, specifically the  $\alpha 5$  and  $\beta 1$  subunits of integrin. The results of this study show that this method is also applicable for identifying CPSCs (Pei *et al.*, 2013).

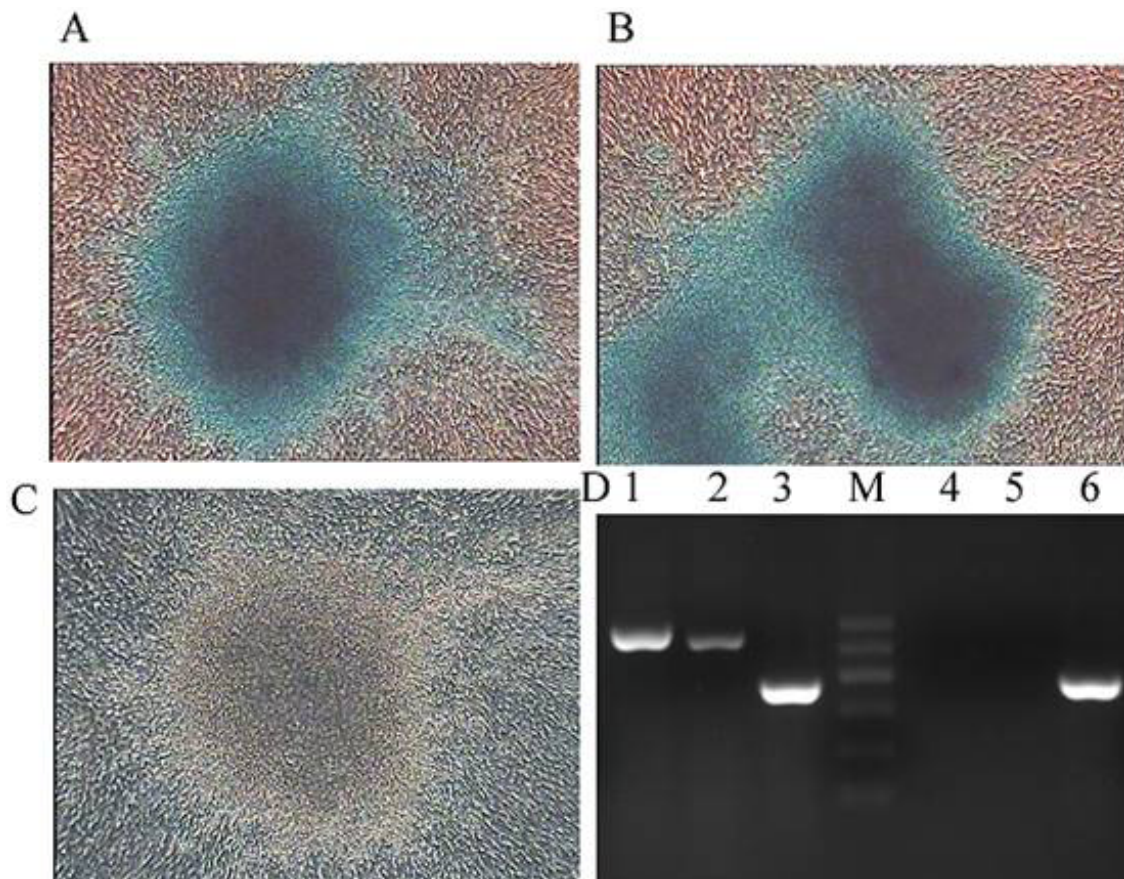


Fig. 6. Chondrogenic differentiation of CPSCs. After induction for 15 days, the cells in some areas aggregate to form clusters, and become larger. A–C, the induced cells were alcian blue positive. (100 $\times$ ) D RT-PCR revealed the expression of the chondrocyte-specific genes lane 1 Vimentin and lane 2 ACAN in cells from the induced group, whereas these genes were not expressed in cells from the control group (lane 4–5). GAPDH (lane 3 and Lane 6) served as the internal control.

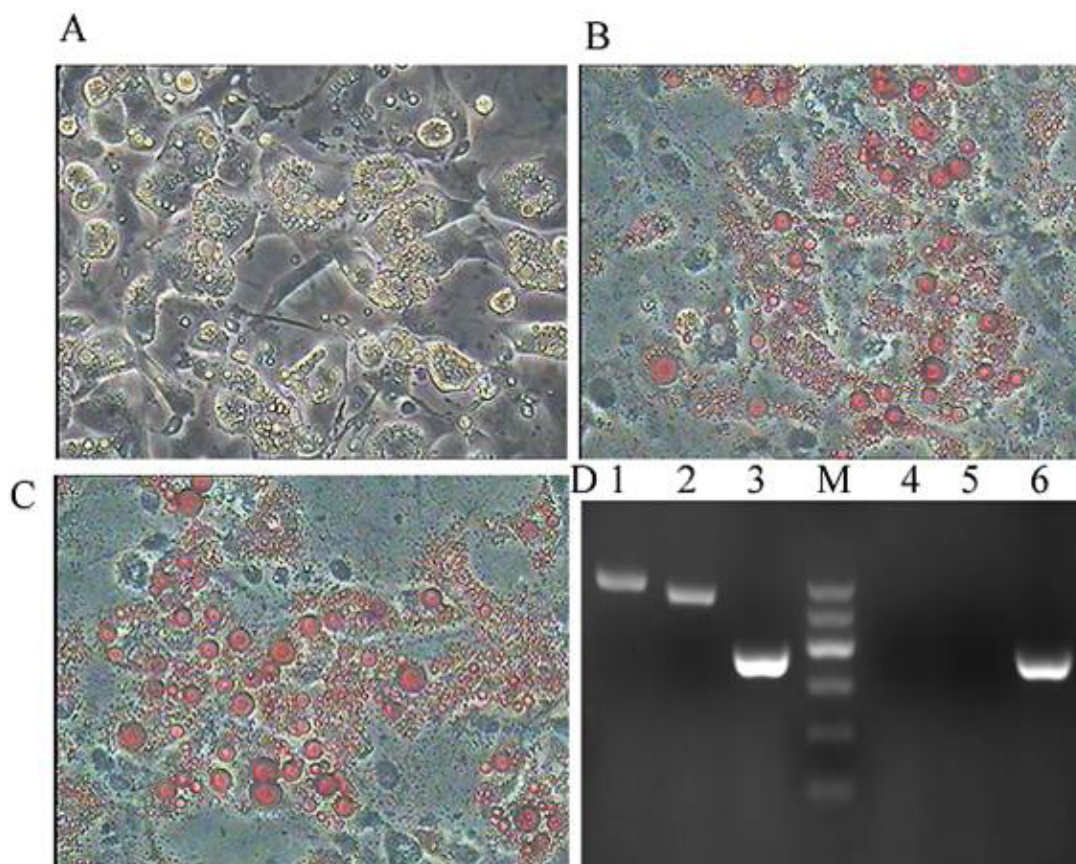


Fig. 7. Adipogenic differentiation of CPSCs. After induction for 15 days, many big bright lipid droplets were observed in the cells. **A–C**, The induced cells were oil red O positive (100 ×). **D**, RT-PCR revealed the expression of the adipocyte-specific genes lane 1 LPL and lane 2 PPAR $\gamma$  in cells from the induced group, whereas these genes were not expressed in cells from the control group (lane 4 and 5). GAPDH served as the internal control (lane 3 and 6).

There is no uniform standard for the identification of CPSCs. At present, the standard is mainly based on the identification criteria for mesenchymal stem cells formulated by the International Society for Cellular Therapy (ISCT), namely: adherence, surface antigen expression, and differentiation in three directions (osteogenesis, adipogenesis, and chondrogenesis) (Quintin *et al.*, 2010). Stem cell surface markers are important indicators for judging whether the cells have stem cell characteristics. We used immunofluorescence and RT-PCR analyses to detect the surface markers of the isolated cells. The results showed that the cells positively expressed FGFR-3, collagen type II, CD44, CD73, CD90, vimentin, Notch1, CD105, and CD106, and negatively expressed the haematopoietic stem cell surface marker CD34. The results of flow cytometry showed that the isolated cells had CD79, CD90, CD105, and CD106 expression rates of above 99%, indicating that the cells have stem cell characteristic (Duenas *et al.*, 2014; Paebst *et al.*, 2014). Among these

markers, Notch1 is an important signalling molecule that regulates stem cell proliferation and differentiation, and is considered to be a marker for labelled stem cells, fibroblast growth factor-3 (FGF-3) has been reported by Robinson as a marker for the specificity of pre-articular cartilage stem cells (Duenas *et al.*, 2014), and collagen type II is secreted and synthesized by chondrocytes; it has a strong affinity for, and can play a role in the growth, proliferation, differentiation, and function of chondrocytes (Duenas *et al.*, 2014). Thus, the cells obtained from articular cartilage have stem cell characteristics. In addition, the CPSCs maintained a high expression rate of these genes during the third passage, suggesting that cartilage-derived stem cells may serve as suitable seed cells for cartilage tissue engineering.

The stem cells can survive only at very low densities (<50/cm<sup>2</sup>), while other cells cannot survive because their densities are too small (Sekiya *et al.*, 2002). Therefore, low-density colony formation analysis was used to verify

whether the clonal populations obtained from these cells have stem cell properties. The abilities of clone formation and multi-directional differentiation are the basic characteristics of stem cells. For this reason, we have carried out experiments testing the clone-formation and multipotential differentiation ability of the cells. The experimental results show that CPSCs have strong colony formation analysis ability and formed obvious monoclonal cell clusters, but their clone formation ability gradually decreases with the increase in the cell generation number. The results of the experiments testing the induction of differentiation in three directions showed that the cells were capable of osteogenic, adipogenic, and chondrogenic differentiation, and further clarify their stem cell characteristics. We constructed the growth curves of the CPSCs from P3, P15 and P25, which were standard S-shaped curves. As the generation increases, the growth rate of the cells is slower.

After multiple passages, CPSCs can maintain their surface markers to retain the cartilage phenotype, which indicates that they have stable cartilage-forming ability and have great potential as seed cells for tissue engineering. However, there are still many problems associated with the clinical application of using CPSCs as seed cells for repairing cartilage defects. First, scientists need to further identify specific surface markers to optimize the screening process for seed cells. Second, Marcus *et al.* (2014) injected CPSCs into the muscles of immunodeficient rats and found that although CPSCs can maintain their phenotype and have a cartilage-producing ability, they do not effectively form cartilage-like tissue. This experiment considers that the cartilage-forming ability of CPSCs is affected by the surrounding environment; however, the cartilage-forming ability of CPSCs *in vivo* needs further investigation. Third, how the differentiation of CPSCs can be controlled *in vivo* and whether these cells will become malignant also pose problems. CPSCs should be further evaluated with regards to biosafety before their clinical application. However, with the in-depth study of CPSCs by scientists, the development of methods to study cartilage tissue pathology and the use of bioengineering methods represent bright prospects for the treatment of cartilage diseases, and may also highlight the importance of CPSCs as a new source of seed cells for tissue engineering.

## CONCLUSIONS

This study demonstrated the presence of stem cells in the cartilage tissue of Peking duck embryos by means of the analysis of cell morphology, cell markers, and biological features. We also showed that CPSCs have the ability to self-renew, and show osteogenic, adipogenic, and

chondrogenic differentiation *in vivo*. This study not only provides a platform for the establishment of a Peking duck CPSC bank, but also proposes a new method to preserve the valuable genetic resources of ducks and other poultry.

### Statement of conflict of interest

The authors have declared no conflict of interests.

## REFERENCES

- Alsalameh, S., Amin, R., Gemba, T. and Lotz, M., 2004. Identification of mesenchymal progenitor cells in normal and osteoarthritic human articular cartilage. *Arthritis Rheum*, **50**: 1522-1532. <https://doi.org/10.1002/art.20269>
- Cui, J.H., Park, S.R., Park, K., Choi, B.H. and Min, B.H., 2007. Preconditioning of mesenchymal stem cells with low-intensity ultrasound for cartilage formation *in vivo*. *Tissue Eng.*, **13**: 351-360. <https://doi.org/10.1089/ten.2006.0080>
- de Luca, P., Kouroupis, D., Vigano, M., Perucca-Orfei, C., Kaplan, L., Zagra, L., de Girolamo, L., Correa, D. and Colombini, A., 2019. Human diseased articular cartilage contains a mesenchymal stem cell-like population of chondroprogenitors with strong immunomodulatory responses. *J. Clin. Med.*, **8**: 423. <https://doi.org/10.3390/jcm8040423>
- Diekmann, B.O., Christoforou, N., Willard, V.P., Sun, H., Sanchez-Adams, J., Leong, K.W. and Guilak, F., 2012. Cartilage tissue engineering using differentiated and purified induced pluripotent stem cells. *Proc. natl. Acad. Sci. U.S.A.*, **109**: 19172-19177. <https://doi.org/10.1073/pnas.1210422109>
- Duenas, F., Becerra, V., Cortes, Y., Vidal, S., Saenz, L., Palomino, J., de Los Reyes, M. and Peralta, O.A., 2014. Hepatogenic and neurogenic differentiation of bone marrow mesenchymal stem cells from abattoir-derived bovine fetuses. *BMC Vet. Res.*, **10**: 154. <https://doi.org/10.1186/1746-6148-10-154>
- Jungmann, P.M., Kraus, M.S., Nardo, L., Liebl, H., Alizai, H., Joseph, G.B., Liu, F., Lynch, J., McCulloch, C.E., Nevitt, M.C. and Link, T.M., 2013. T(2) relaxation time measurements are limited in monitoring progression, once advanced cartilage defects at the knee occur: Longitudinal data from the osteoarthritis initiative. *J. Magn. Reson. Imag.*, **38**: 1415-1424. <https://doi.org/10.1002/jmri.24137>
- Kreuz, P.C., Gentili, C., Samans, B., Martinelli, D., Kruger, J.P., Mittelmeier, W., Endres, M., Cancedda, R. and Kaps, C., 2013. Scaffold-assisted cartilage tissue engineering using infant chondrocytes from human hip cartilage. *Osteoarthritis Cartilage*,

- 21: 1997-2005. <https://doi.org/10.1016/j.joca.2013.09.007>
- Marcus, P., de Bari, C., Dell'Accio, F. and Archer, C.W., 2014. Articular chondroprogenitor cells maintain chondrogenic potential but fail to form a functional matrix when implanted into muscles of SCID mice. *Cartilage*, **5**: 231-240. <https://doi.org/10.1177/1947603514541274>
- Naderi-Meshkin, H., Andreas, K., Matin, M.M., Sittinger, M., Bidkhorji, H.R., Ahmadiankia, N., Bahrami, A.R. and Ringe, J., 2014. Chitosan-based injectable hydrogel as a promising in situ forming scaffold for cartilage tissue engineering. *Cell Biol. Int.*, **38**: 72-84. <https://doi.org/10.1002/cbin.10181>
- Paebst, F., Piehler, D., Brehm, W., Heller, S., Schroeck, C., Tarnok, A. and Burk, J., 2014. Comparative immunophenotyping of equine multipotent mesenchymal stromal cells: An approach toward a standardized definition. *Cytometry A*, **85**: 678-687. <https://doi.org/10.1002/cyto.a.22491>
- Pei, M., He, F., Li, J., Tidwell, J.E., Jones, A.C. and McDonough, E.B., 2013. Repair of large animal partial-thickness cartilage defects through intraarticular injection of matrix-rejuvenated synovium-derived stem cells. *Tissue Eng. Part A*, **19**: 1144-1154. <https://doi.org/10.1089/ten.tea.2012.0351>
- Pelttari, K., Winter, A., Steck, E., Goetzke, K., Hennig, T., Ochs, B.G., Aigner, T. and Richter, W., 2006. Premature induction of hypertrophy during *in vitro* chondrogenesis of human mesenchymal stem cells correlates with calcification and vascular invasion after ectopic transplantation in SCID mice. *Arthritis Rheum*, **54**: 3254-3266. <https://doi.org/10.1002/art.22136>
- Peng, H. and Huard, J., 2004. Muscle-derived stem cells for musculoskeletal tissue regeneration and repair. *Transpl. Immunol.*, **12**: 311-319. <https://doi.org/10.1016/j.trim.2003.12.009>
- Puculek, M., Baj, J., Portincasa, P., Sitarz, M., Grochowski, C. and Radzikowska, E., 2020. The morphology and application of stem cells in digestive system surgery. *Folia Morphol. (Warsz)*, <https://doi.org/10.5603/FM.a2020.0024>
- Quintin, A., Schizas, C., Scaletta, C., Jaccoud, S., Applegate, L.A. and Pioletti, D.P., 2010. Plasticity of fetal cartilaginous cells. *Cell Transpl.*, **19**: 1349-1357. <https://doi.org/10.3727/096368910X506854>
- Reverte-Vinaixa, M.M., Joshi, N., Diaz-Ferreiro, E.W., Teixidor-Serra, J. and Dominguez-Oronoz, R., 2013. Medium-term outcome of mosaicplasty for grade III-IV cartilage defects of the knee. *J. Orthop. Surg. (Hong Kong)*, **21**: 4-9. <https://doi.org/10.1177/230949901302100104>
- Sekiya, I., Larson, B.L., Smith, J.R., Pochampally, R., Cui, J.G. and Prockop, D.J., 2002. Expansion of human adult stem cells from bone marrow stroma: Conditions that maximize the yields of early progenitors and evaluate their quality. *Stem Cells*, **20**: 530-541. <https://doi.org/10.1634/stemcells.20-6-530>
- Tang, C., Jin, C., Li, X., Li, J., Du, X., Yan, C., Lu, S., Wei, B., Xu, Y. and Wang, L., 2019. Evaluation of an autologous bone mesenchymal stem cell-derived extracellular matrix scaffold in a rabbit and minipig model of cartilage repair. *Med. Sci. Monit.*, **25**: 7342-7350. <https://doi.org/10.12659/MSM.916481>
- Veronesi, F., Maglio, M., Tschon, M., Aldini, N.N. and Fini, M., 2014. Adipose-derived mesenchymal stem cells for cartilage tissue engineering: state-of-the-art in *in vivo* studies. *J. Biomed. Mater. Res. A*, **102**: 2448-2466. <https://doi.org/10.1002/jbm.a.34896>
- Viti, F., Scaglione, S., Orro, A. and Milanese, L., 2014. Guidelines for managing data and processes in bone and cartilage tissue engineering. *BMC Bioinformatics*, **15**(Suppl 1): S14. <https://doi.org/10.1186/1471-2105-15-S1-S14>